Socially induced plasticity of the posterior tuberculum and motor behavior in zebrafish (*Danio rerio*)

Faith K Heagy, Katie N Clements, Carrie L Adams, Elena Blain, Fadi A Issa*

Department of Biology, East Carolina University, Greenville, NC 27858

*Corresponding author: Dr. Fadi A. Issa

East Carolina University, Department of Biology, Life Sci. & Biotech. Bldg., 101 E. 10th ST.,

Greenville, NC 27858, USA

Phone: 252-328-5446 Email: issaf14@ecu.edu

Keywords: Aggression, dopamine, diencephalon, Mauthner neuron, social dominance,

zebrafish

Abstract

Social dominance is prevalent throughout the animal kingdom. It facilitates the stabilization of social relationships and allows animals to divide resources according to social rank. Zebrafish form stable dominance relationships that consist of dominants and subordinates. Although social-status-dependent differences in behavior must arise due to neural plasticity, mechanisms of how neural circuits are reconfigured to cope with social dominance are poorly described. Here, we describe how the posterior tuberculum nucleus (PT), which integrates sensory social information to modulate spinal motor circuits, is morphologically and functionally influenced by social status. We combined non-invasive behavioral monitoring of motor activity (startle escape and swim) and histological approaches to investigate how social dominance affects the morphological structure, axosomatic synaptic connectivity, and functional activity of the PT in relation to changes in motor behavior. We show that dopaminergic cell number significantly increases in dominants compared to subordinates, while PT synaptic interconnectivity, demonstrated with PSD-95 expression, is higher in subordinates compared to dominants. Secondly, these socially induced morphological differences emerge after one week of dominance formation and correlate with differences in cellular activities illustrated with higher phosphor-S6 ribosomal protein expression in dominants compared to subordinates. Thirdly, these morphological differences are reversible as the social environment evolves

and correlates with adaptations in startle escape and swim behaviors. Our results provide new insights of the neural bases of social behavior that may be applicable to other social species with similar structural and functional organization.

Introduction

Decision-making is critical for animal survival. In social species, decision-making is context dependent driven, in part, by social cues as animals compete for dominance. During social interactions, neural networks integrate social information and drive spinal circuits to produce adaptive behavior. One common view is that neural circuits underlying reflexive behaviors such as those involved in escape or freezing are "hard-wired" and resistant to physiological plasticity (Manoli et al., 2006). Conversely, social behaviors involving learning and memory that change as the social environment evolves are mediated by flexible circuits that allow for more adaptive behavioral responses (Anderson et al., 2014; Stagkourakis et al., 2020; Yavas et al., 2019). However, it is likely that hard-wired and flexible neural circuits overlap or share common elements that maximize behavioral adaptations (Stagkourakis et al., 2020). Although, social status-dependent plasticity of neural circuits involved in reflexive and adaptive behaviors has been extensively investigated in various systems (Edwards and Kravitz, 1997; Jung et al., 2020; Müller et al., 2008; Whitaker et al., 2021), our knowledge of how social dominance influence the morphological and functional organizations of brain circuits involved in motor control remains poorly understood.

Decision-making circuits implicated in social regulation have been extensively studied in several mammalian and teleost fish species (Filby et al., 2010; O'Connell and Hofmann, 2011; O'Connell and Hofmann, 2012b; O'Connell and Hofmann, 2012b). Several brain regions that include the diencephalon, hypothalamus and telencephalon form neural nodes that play important roles in social aggression. Within these regions, an upregulation of specific genes are linked to aggression, including *slc6a3*, which codes for the dopamine active transporter (DAT) and dopamine type 2 receptor (*drd2*) (Chen et al., 2005). The elevated expression of *slc6a3* is of particular interest given the regulatory involvement of dopaminergic pathways in social anxiety, depression, motivation, and aggression (Filby et al., 2010; Schwab-Reese et al., 2020). Being that it is well established that aggressive interactions have profound physiological effects on many animals (Chen et al., 2005; Filby et al., 2010; Schwab-Reese et al., 2020), we aimed to provide insight into how the cellular mechanisms that underlie changes in decision-making for motor circuits are modified in a status-dependent manner.

Zebrafish (*Danio rerio*) have emerged as a suitable model organism to study the neurobiology of social behavior. Zebrafish shoal and communally engage in social agonistic interactions to form stable social dominance relationships (Oliveira et al., 2011; Miller et al., 2017; Clements et al., 2018; Clements et al., 2023). These agonistic interactions are driven by hormonal and neural regulation of brain nuclei involved in social regulation (O'Connell and

Hofmann, 2012a; O'Connell and Hofmann, 2012b). Specifically, the dopaminergic system is widely known for its neuromodulatory regulation of motivated behavior, aggression, and regulation of motor activity (Clemens et al., 2006; Haehnel-Taguchi et al., 2018; Weitekamp et al., 2017). Of particular importance, the posterior tuberculum (PT), within the ventral diencephalon, forms a functional network that receives visual information from the optic tectum (Mu et al., 2012; Vernier and Wullimann, 2009; Yamamoto et al., 2017), integrates, and relays such information via ascending projections to the striatum and descending projections into the spinal cord (Ryczko et al., 2013). Within the PT, the posterior tuberculum anterior rostral (PTar) and posterior tuberculum anterior caudal (PTac) neural cluster project posteriorly into the mesencephalic region to directly modulate the startle escape and swim circuits and indirectly by modulating hindbrain glycinergic nuclei (Haehnel-Taguchi et al., 2018; Mu et al., 2012; Ryczko et al., 2013), the excitability of which is socially influenced (Orr et al., 2021; Clements et al., 2023). One distinguishing feature of PTar/PTac neurons is their large almond shaped somata by comparison to other neighboring DA neurons (e.g., posterior tuberculum posterior group, PTp), which facilitates their identification. Collectively, given the importance of visual communication during agonistic interactions along with the input/output structural organization of the PT suggests propensity to socially mediated plasticity as animals fight for social dominance. However, the effects of social dominance on the morphological and functional organization of the PT and downstream motor circuits remains unknown.

Previously, we have demonstrated that the startle and swim behaviors are socially regulated. After two weeks of continuous social interactions, dominant animals increase their swimming activity and become less likely to startle, while subordinates display the opposite behavior pattern by reducing their swimming activity and increasing their startle sensitivity (Miller et al., 2017). Although the cellular mechanisms underlying this status-dependent shift in motor activity remain unknown, these changes are likely driven, in part, by descending neuromodulatory input from the PTar/PTac cluster into the spinal cord to modulate startle and swim behaviors (Haehnel-Taguchi et al., 2018; Mu et al., 2012). This notion is supported by recent evidence showing that dopaminergic regulation of the startle escape and swim behaviors is socially driven to modulate the excitability of the startle escape and swim circuits in a status-dependent manner (Clements et al., 2023). This lends credence to the hypothesis that social dominance may affect the morphological and functional activity of the PTN. Here, we tested this hypothesis by examining the time course during which adaptations in motor activity emerge and their relation to PTN morphological and functional plasticity. We show that the number of DAT+ neurons in the PTar/PTac neural cluster increases in dominant animals compared to social subordinates, while synaptic connectivity is higher in subordinates compared to dominants. These socially induced morphological differences develop between 9-14 days post dominance formation and correlate with status-dependent cellular functional activities in phosphor-S6 ribosomal protein (PS6) expression. PS6 detects ribosomal proteins

that were recently phosphorylated indicative of increased protein synthesis and enhanced cellular activity (Wayne et al., 2023). Finally, we show that these status-dependent differences are highly plastic and reversible if animals were provided opportunities for social rise or induced into social fall.

Methods & Materials

Animal care and housing

Zebrafish transgenic line with specific green fluorescent protein expression in DAT neurons Tg(dat:GFP) was provided by Dr. Timothy Erickson and maintained at the core aquatic animal facility in grouped-housed tanks consisting of 15-20 adult zebrafish of mixed sex. The facility was kept at 28 °C under a 10 h dark/14 h light cycle. Fish were fed live brine shrimp and pellet food twice daily. All experiments were conducted according to guidelines approved by East Carolina University's Institutional Animal Care and Use Committee.

Behavioral isolation, pairing, and observation process

Although female zebrafish engage in agonistic interactions and form short-term dominance relationships (Teles and Oliveira, 2016), they undergo diurnal ovulation with the corresponding hormonal fluctuations that lead to unstable levels of aggressive activity and instability of dominance relationships. Given that the objective of our study was to examine the long-term consequences of stable social dominance on PTar/PTac morphological and functional activity, we limited the scope of the study only to adult male zebrafish. Adult male Tg(dat:GFP) zebrafish, ranging from 3-12 months old were isolated physically and visually from conspecifics for one week in 23x13x6 cm individual tanks, to minimize prior social experience. Following isolation, two male fish of equal size, age, and identical genetic background were paired continuously for either 7, 9, or 14 days. Aggressive interactions were observed daily for 2-3 minutes at mid-day, and the number of attacks and retreats were quantified as described previously to ensure dominance stability (Miller et al., 2017). When paired, zebrafish form dominance relationships within an hour after pairing by engaging in ritualized agonistic interactions. Social dominance was determined daily for each pair based on the total number of aggressive attacks (biting and chasing) and defensive retreats. Fish with a high number of attacks were considered dominants while those that retreated from the attacks were considered subordinates. As dominance matures after day 1, the level of aggressive activities declines whereby only dominants attack while subordinate fish retreat. None of the pairs tested experienced social reversals during the first two weeks of interactions.

Startle escape and swim behavioral testing.

Using a non-invasive approach, the muscular electric field potentials during M-cell mediated c-start escape and swim behaviors were recorded as described in detail elsewhere (Issa et al.,

2011; Miller et al., 2017; Clements et al., 2023). Muscular field potentials were amplified (x1000, AM-Systems, model 1700) and low-pass filtered at 300 Hz and high-pass filtered at 1 KHz before signals were digitized using Digidata 1550 digitizer and stored on a personal computer (Axoscope software, Molecular Devices). After behavioral observations on days 7, 9, or 14, the fish were placed individually in a bath electrode chamber and allowed to acclimate for 30 minutes before testing. Following acclimation, one minute of spontaneous swimming activity was recorded. To test escape response sensitivity, auditory pulses at increasing decibels between 0-100 dB re 20 μ Pa were randomly delivered (1 1/2 minutes ISI) with 5dB increments. 1ms square sound pulses were generated using Audacity software. Stimuli amplitudes were randomized to prevent learning and desensitization effects. Each decibel was repeated 3 times. Startle responses that occurred within 15 ms or less of the auditory pulse was considered M-cell mediated escape response (Korn and Faber, 2005; Issa et al., 2011; Marsden and Granato, 2015). Escape probabilities were determined among all social groups with all values provided as mean and ±SEM. Swim burst analysis using Clampfit software was completed by detecting any burst if they are larger than 12 mV in total amplitude and the duration of the burst needed to be in the range of 50-200 ms to be considered a swim burst. Instantaneous frequencies and average number of bursts per one minute were tabulated. All data was graphed using GraphPad Prism software.

Reversal behavioral experiments

Males were isolated for one week then paired continuously for 14 days. On day 14, two dominants from separate pairs were size matched to form a new (Dominant vs. Dominant) pair. Similarly, subordinates from separate pairs were crossed to form new (Subordinate vs. Subordinate) pairs. The new pairs were kept together continuously for an additional 14 days to allow formation of new dominance relationships (Total 28 days of pairing). Isolation, pairing, and behavioral testing of startle sensitivity and swimming activity was carried out as described earlier.

Brain tissue extraction, preparation, and slicing

Immediately following behavioral experiments, animals were euthanized in 0.2% MS-222, then the brains were extracted and placed in 4% paraformaldehyde overnight at 4°C. The following day, brains were washed repeatedly for 25 minutes in 1% PBS. Brain tissue were incubated overnight in 30% sucrose in 4°C for cryoprotection. Brains were embedded in OCT filled molds, oriented sagittally, then flash frozen in liquid nitrogen. Embedded brain tissues were sliced at 30 µm using a cryostat (Microm HM 550) and slices were placed onto a Superfrost Plus Microscope slides (Fisher Scientific). Brain slices were allowed to dry completely onto the slides in dark containers for 10 minutes prior to staining.

Immunohistochemistry

Post synaptic density-95 (PSD-95) (Abcam #Ab18258) and Phospho-S6 Ribosomal Protein (Ser235/236) antibody (Cell Signaling # 2211) for PS6 staining were used and previously tested and confirmed in zebrafish (Brenet et al., 2019; He et al., 2021). Slices were washed 3-4 times for 5 minutes each in 1% phosphate buffer solution (PBS) then placed in 5% bovine serum and 2% goat serum blocking buffer (1-2 hours) following cryo-sectioning. Another series of PBS washes (3-4 times for 5 minutes) were performed, and slices were stained with a rabbit polyclonal anti-PSD-95 primary antibody at a concentration of 1:200. PS6 experiments, the tissue was incubated at a concentration of 1:600. Slides are then incubated overnight at 4°C. Following primary antibody incubation, additional 3-4 PBS washes were performed, and slices incubated for 1-2 hours at room temperature in goat anti-rabbit Alexa Fluor-555 secondary antibodies (Invitrogen #A21428) diluted at a 1:500 concentration. Secondary antibodies were washed in PBS (3-5x) then slides were mounted with one drop of Antifade gold reagent protectant (Invitrogen #P36980). Slides were cured in the fridge for 24 hours then sealed.

Imaging acquisition and analysis

Confocal images were obtained using a Carl Zeiss LSM 800 confocal microscope equipped with 40x oil objective lens. To standardize acquisition across animal groups, acquisition mode settings were kept constant across conditions. Once imaging was completed, confocal stacks were imported and analyzed using Imaris software (Oxford Instruments, ver. 9.3) for automated cell count, colocalization, fluorescence intensity, and volumetric analysis. Cell count of PTar, PTac, PTp, lateral recess, and paraventricular organ posterior part B (PVOpB) neurons was conducted by selecting either the spots or cell surface functions. All image analysis was conducted blind and cross checked by multiple individuals. Fluorescence intensity analysis was conducted in ImageJ. Fluorescence intensity of PTar/PTac cells was measured by calculating the corrected total cell fluorescence (CTCF) according to the following equation: CTCF = integrated density – (cell area x background average fluorescence). CTCF of a minimum of 10 cells per brain slice was measured. PS6 expressing cells with either CTCF <6K (low signal to noise threshold) or >800K (saturation of fluorescence) were excluded from analysis. Analyzed data was exported and tabulated into Excel and graphed in Prism (GraphPad, ver. 3) software.

Statistical Analysis

Prism was used to generate all graphs and statistical results. Statistical analysis was performed using One-Way ANOVA test with Kruskal-Wallis multiple comparison post-test, two-tailed; data met requirement of normal distribution, and no data points were excluded from analysis for any of the results presented. To compare M-cell startle escape response probability among the social groups, the data was curve fitted with a Boltzmann Sigmoidal curve fit with a non-linear regression. One-Way ANOVA tests were performed to compare average number of swim bursts

per minute, and the number of PTac and PTar neurons at day 7, 9, and 14 of social pairing for each phenotype. A paired t-test was performed on soma volumetric differences between PTar, PTac and PTp cells as well as comparing cell number across experimental conditions relative communal fish (controls). Control fish were males selected from tanks in which 15-20 fish of mixed sex were group-housed. The selected fish were siblings of the experimental group fish. The controls were of similar size, age, and genetic background as the experimental group fish. Chi-square analysis was performed on PSD-95 expression differences among social phenotypes. Statistical significance level was set to p<0.05. The in the R statistical environment was used to conduct principal component analysis (PCA) using the *prcomp*() function (R version 4.3.3, 2024; R Studio version 2023.12.1+402) (R Code Team, 2024). We used packages ggfortify (Tang et al., 2016), factoextra (Kassambara and Mundt, 2020), ggplot2 (Wickham, 2016) to visualize the results. The PCA was used to examine and visualize clustering of individuals according to social status groups based on the set physiological and behavioral variables measured. Each sample is represented as a point (or projection) and arrows represent the correlations of each variable to the principal components.

Results

Sensitivity of the M-cell mediated startle response is socially regulated

Prior work demonstrated that after 14 days of interactions, patterns of motor activity shift according to social rank whereby dominants increase their swimming activity and reduce their startle sensitivity, while subordinates reduce their swimming and increase their startle sensitivity (Miller et al., 2017). However, the time course during which these behavioral adaptations emerge and their relation to changes in brain morphology have not been examined. We hypothesized that during the early periods of dominance formation (days 7 and 9) there will be no social status-dependent differences since social relationships have not yet been matured. To test this hypothesis, we measured the animals' startle escape sensitivity and swim behavior in dominants and subordinates at 7, 9 and 14 days of social interactions (Figure 1). We found that the sensitivity of startle escape among all groups on day 7 and day 9 showed no significant differences (Figure 1A; day 7: communals n=6, dominants n=9, subordinates n=9; day 9: communals n=6, dominants n=6, subordinates n=6) though there was a diverging trend in startle response where subordinates were slightly more sensitive and dominants were not as responsive. Those differences became progressively more pronounced and statistically different by day 14 (One-Way ANOVA, Kruskal-Wallis post-test, com vs. sub [85dB] p=0.0434, [87dB] com vs. dom p=0.053, dom vs. sub [90dB] p=0.0226, communals n=6, dominants n=6, subordinates n=6).

As with startle escape response, when we measured swimming activity among the three social groups, we found a corresponding change in the swimming pattern that emerged after 9

days and became significant by day 14 post pairing (Figure 1B). We found that dominants and subordinates did not vary in spontaneous swim activity on days 7 and 9, but by day 14 subordinates significantly decreased their swimming activity (Figure 1C. One-Way ANOVA, Kruskal-Wallis post-test. Day 7: p=0.440; communals n= 7, dominants n= 11, subordinate n= 11. Day 9: p=0.8461; communals n=7, dominants n=6, subordinate n=6. Day 14: p=0.0142; communals n= 7, dominants n= 8, subordinate n= 8). These results show although social dominance may be established quickly within the first week of social interactions, social statusdependent differences in motor activity emerge later between 9- and 14-days as dominance matures.

Social status affects PT cell number

PT dopaminergic nucleus integrates sensory social information and relays those signals to spinal cord circuits including the M-cell startle escape circuit. Given the observed differences in escape sensitivity between dominants and subordinates, we hypothesized that the PTar/PTac cluster within the PT is prone to socially induced plasticity. First, we quantified the total number of PT cells in socially dominant, subordinate, and communal controls between days 7-14 post pairing (Figure 2). As noted, the PT consists of several DA expressing nuclei, and only the PTar/PTac cluster has large and almond shaped cells that project and innervate spinal cord targets. To ensure accurate identification of the PTar/Ptac, we measured and compared their soma volume to those of neighboring PT nuclei (e.g., PTp) (Figure 2B, C). We found that the average soma volume of PTar/PTac cluster was significantly larger compared to the PTp nucleus, consistent with a prior report (Figure 2C, t-test, P<0.0001, communal PTar/PTac: n= 27, PTp n= 28) (Haehnel-Taguchi et. al, 2018). But we found no differences in PTar/PTac soma volume among the three social phenotypes, nor was there a correlation in soma volume between dominant and subordinate pairs (Figure 2D, One-Way ANOVA, Kruskal-Wallis posttest, p=0.5008; communal n=9, dominants n=9, subordinates n=9). Next, we compared the number of PTar/PTac cells on days 7, 9 and 14 among the three social phenotypes. On days 7 and 9, communals had a significantly higher number of cells compared to subordinates, but there were no differences between communal vs. dominants and dominants vs. subordinates (Figure 2E, One-Way ANOVA, Kruskal-Wallis post-test, Day 7: p=0.0036; communal n=10, dominants n=7, subordinates n=7; Day 9: p=0.0088; Communal n=10, Dominants n=6, subordinates n=6). However, by day 14, the number of cells between dominants and subordinates became statistically significant (Figure 2E, Movie 1; One-Way ANOVA, Kruskal-Wallis post-test, p=0.0013; communals n=10, dominants n=9, subordinates n=9). Interestingly, in dominant animals, the average number of PTar/PTac neurons gradually increased over time and became significantly higher by day 14 compared to day 7 (Figure 2F; One-Way ANOVA, Kruskal-Wallis post-test, p= 0.0116, Communals n= 10, dominants day 7 n=7; day 9 n=6, day 14 n=9). In subordinates, the number of cells remained consistently lower relative to communals

(Figure 2G; One-Way ANOVA, Kruskal-Wallis post-test, p=0.0015, subordinates day 7 n=7; day 9 n=6, day 14 n=9). These results show that the PT is prone to social plasticity. Social pairing with a new animal induces a decline in the number of PTar/PTac cells (One-Way ANOVA, Com vs. Iso. p>0.05), but dominants quickly recover while subordinates do not.

To determine if the effects of social dominance on dopaminergic nuclei is specific to the PTar/PTac or extend to proximate dopaminergic nuclei, we examined the lateral recess and PVOp nuclei that are adjacent to the PT (Refer to Figure 2A for a reference). The lateral recess and PVOp axonal projections are local and are thought to be involved in hormonal homeostatic regulation; thus, are unlikely to be affected by social dominance (Haehnel-Taguchi et al., 2018). To test this hypothesis, we quantified the number of DAT+ cells in the lateral recess and PVOp nuclei (Table 1). We found no statistical differences among all social groups in the PVOp and lateral recess regions (table 1). This result suggests that the effect of social dominance on the PT is likely specific to dopaminergic nuclei that are involved in social regulation.

Differences in motor activity and plasticity of PT cell number are not innate

The gradual divergence in PT cell number during the two weeks of social interactions suggested that social factors rather than innate differences underly the observed results (Figure 3E). To investigate the robustness of social influence on PT morphology, we hypothesized that reversal in social conditions would correlate with reversal in motor behavior and PT cell number. We tested this hypothesis by pairing dominants together to form new pairs (dom vs. dom) and subordinates together to form new pairs (sub vs. sub) and allowed the new pairs to establish social relationships for an additional 14 days of interactions (Figure 3A). Under this scenario, dom vs. dom pairs, one of the animals would remain dominant while its partner would become a subordinate. Conversely, in the sub vs. sub pairs, one of the animals would become dominant while its counterpart would remain a subordinate. After two weeks of social interactions, we measured the animals' startle escape sensitivity, swimming activity, and number of PTar/PTac cells (Figure 3 B-E).

In the dom/dom pairs, the sensitivity of the startle response of the descending subordinates (D \rightarrow S) did not shift significantly compared to their dominant counterparts (D \rightarrow D) (Figure 3B). However, sensitivity of the startle response differed significantly between dominants and subordinates in the sub/sub pairs. The sensitivity of the startle response of the ascending dominants (S \rightarrow D) declined significantly compared to their subordinate counterparts (S \rightarrow S) (Figure 3B; two-tailed paired t-test [85dB] p=0.0313, t=4.382 df=6; [87dB] p=0.0049, t=4.336 df=6; n=7 pairs). Interestingly, the dom/dom pairs displayed higher aggressive activity and mortality rate (5 pairs were excluded from analysis due to mortality) compared to the sub/sub pairs.

Next, we measured spontaneous swimming activity. In the dom/dom pairs, swimming frequency of dominants that lost their ranks and became subordinates (D \rightarrow S) declined

compared to their dominant counterparts (D \rightarrow D), but the decline was not statistically significant (Figure 3C, two-tailed paired t-test p=0.1910; t=1.512 df=5, n=6 pairs). However, in the sub/sub pairs, swimming frequency of subordinates that ascended and became dominants (S \rightarrow D) increased significantly compared to their subordinate counterparts (S \rightarrow S) (Figure 3C; two-tailed paired t-test p=0.0192; t=3.403 df=5, n=6 pairs). Interestingly, the increase in swimming frequency among the dominants (S \rightarrow D) in the sub/sub pairs rose nearly to the level of those of dominants in the dom/dom pairs (D \rightarrow D) and became statistically indistinguishable (Figure 3C; two-tailed unpaired t-test p=0.187; t=1.417 df=10, n=6 animals). Finally, comparison in the swimming frequency between dominants in the dom/dom pairs relative to the subordinates in the (sub vs. sub) pairs showed significant differences (Figure 3C; two-tailed unpaired t-test p=0.003; t=3.886 df=10, n=6 animals), but there were no significant differences between the subordinates in the dom/dom pairs compared to the subordinates in the sub/sub pairs (Figure 3C; two-tailed unpaired t-test p=0.3665, t=0.9459 df=10, n=6 animals).

Finally, we examined the effect of social reversal on the number of PTar/PTac cells. In the dom/dom pairs, the number of PTar/PTac cells in dominants that lost their ranks and became subordinates (D \rightarrow S) declined significantly compared to their dominant counterparts (D \rightarrow D) (Figure 3E, two-tailed paired t-test, p=0.0079; dominants n=6, subordinates n= 5). In the sub/sub pairs, we found that the number of PTar/PTac cells in dominants that ascended from submissive status (S \rightarrow D) increased significantly compared to their subordinate counterparts (S \rightarrow S) (Figure 3E, two-tailed paired t-test, p=0.0057; dominants n=6, subordinates n= 6). Collectively, the results show that PT nucleus and motor activity are socially regulated and highly plastic as animal rise and fall in dominance.

Social status affects synaptic connection of the PT cells

The PT nucleus forms a functional network with extensive synaptic connectivity among its neurons. Cellular gain or loss is likely to impact its structural and functional organization. However, homeostatic mechanisms may play a significant role ensuring continued network functionality. We hypothesized that the observed differences in PT cell numbers may lead to compensatory axosomatic connectivity to maintain PT functional integrity. We tested this hypothesis by staining for PSD-95 synaptic marker (Figure 4, Movie 2). A ratio for each animal was computed by taking the total number of PTar/PTac cells that express PSD-95 divided by the total number of PTar/PTac cells. Using the average ratios of each social group, a Chi-square analysis was performed comparing all social phenotypes. Surprisingly, on average, 21% (SD=0.061, n=6) of PT neurons expressed PSD-95 in dominants, which is significantly lower compared to subordinates that averaged 46% (SD=0.0542, n=6) of PT neurons expressed PSD-95 (Chi-square:14.0276, p=0.0002) (Figure 4B). Communals average PT PSD-95 expression was 27% (SD=0.0957, n=7) and was not statistically different from dominants but was significantly different from subordinates (communal-dominants comparison: Chi-square: 0.9868, p=0.3205;

communal-subordinates comparison: Chi-Square: 7.7877, p=0.0053) (Figure 4B). Overall, the results show that despite a decline in overall PTar/PTac cell number, subordinates have more PT cells that express PSD-95 compared to communals and dominants.

Social status-dependent differences in PS6 expression

Next, we tested the hypothesis that status-dependent morphological differences lead to functional differences in neuronal activity. We rationalized that the PT is a network that must maintain its functional integrity as its morphological architecture adapts to evolving social conditions. We tested this hypothesis by measuring PS6 expression in the PTar/PTac neurons. In contrast to immediate early genes markers (e.g., c-fos and erg1) that detect recent changes in gene expression at the level of transcription, PS6 detects ribosomal proteins that are phosphorylated in the previous ~ 1 h. The increase in phosphorylated ribosomes is tied to increased protein synthesis. Thus, PS6 is a useful marker to measure changes in neural activity (Ruvinsky and Meyuhas, 2006; Maruska et al., 2020; Wayne et al., 2023). We found that PTar/PTac expression of PS6 was significantly higher in dominants compared to subordinates and communal controls (One-Way ANOVA test with Kruskal-Wallis multiple comparison posttest; P=0.0111; communals n=5, dominants n=8, subordinates n=8) (Figure 5D, Movie 3). Moreover, PS6 fluorescence intensity was significantly lower in subordinates compared to dominants and communal fish, but there were no differences between communal and dominants (One-Way ANOVA test with Kruskal-Wallis multiple comparison post-test; P=0.0147) (Figure 5E). The results suggest that morphological plasticity induced by social subordination leads to functional differences in PT activity pattern.

To examine how physiological and behavioral differences correlate with social status, we conducted a multivariate principal component analysis (PCA) (Fig. 6). The first two principal components explained about 74% of the variance. The dominant individuals clustered together where the variables swimming activity and PTN cell number were negatively correlated and loaded strongly to the PC1 axis. In contrast, the subordinate individuals clustered together, where the variable PSD-95 was positively correlated and strongly loaded to the PC1 axis. The communal individuals clustered along PC2, where the variable PS6 intensity was positively correlated and loaded strongly along the PC2 axis. These PCA results confirm the ANOVA results highlighting a strong separation between PTN cell number and PSD-95 according to social status (Fig. 6A & B). Collectively, the multivariate analysis revealed distinct clusters between dominants and subordinates emphasizing the divergence in physiological and behavioral activities as animals ascend or descend in social rank.

Discussion

The PT receives sensory cues from the Optic tectum and integrates and relays social information to the spinal cord to modulate motor activity. Here, we examined the effects of

social status on the startle escape and swim behaviors and how behavioral adaptations correlate with PTN morphological plasticity. Three principal conclusions can be drawn from this study. First, as social dominance solidifies, the behavior patterns of zebrafish diverge according to social rank. Dominant animals increase their swimming activity and reduce their startle escape sensitivity; subordinates reduce their swimming behavior and increase their startle sensitivity. Secondly, these status-dependent differences correlate with morphological changes in PT cell number, synaptic interconnectivity, and activity. Time course experiments suggest that social dominance promotes proliferation in PT cell number, and those differences emerge after 9 days post dominance formation; while social subordination may lead to neuronal loss. Thirdly, socially driven plasticity of PT cell number is reversible suggesting adaptation in motor behaviors and PT function.

Prior evidence points to possible functional consequences of status-dependent differences in PT morphological architecture on motor activity. Clements and colleagues (2023) have shown that DA signaling indirectly modulates M-cell excitability by regulating glycinergic inputs to inhibit M-cell excitability. Thus, activation of the intermediate glycinergic inhibitory input leads to an inhibition of startle sensitivity. Interestingly, the authors demonstrated that increased dopaminergic signaling coupled with increased dopamine receptor type 1 (Drd1) expression by glycinergic neurons strengthens the dopaminergic-to-glycinergic pathway to reduce M-cell excitability in dominants. Thus, an increase in PTar/PTac cell number and elevated expression in PS6 activity are likely to increase dopaminergic release to inhibit startle escape in dominants, which is consistent with the current model. In subordinates, having fewer PT cells would reduce dopaminergic signaling, the consequences of which is likely to disinhibit the M-cell and increase startle sensitivity. This is consistent with the reduced expression of PS6 in subordinates which likely leads to decreased synthesis of dopaminergic signaling associated proteins (Figure 5). Further studies examining synaptic transmission between dopaminergic and glycinergic neurons will be necessary to conclusively demonstrate that dopaminergic proliferation leads to increased synaptic communication. Collectively, the results show that the PT is prone to social regulation by undergoing biochemical and morphological plasticity as animals adapt to new social conditions.

The cellular mechanisms underlying the morphological differences in PTar/PTac remain unresolved, but our results hint to two distinct possibilities that guides future studies: neurogenesis during social rise, and cellular loss because of social submission. The adult zebrafish brain continuously regenerates DA neurons within the diencephalon (Schmidt et al., 2013; Lindsey et al., 2017; Caldwell et al., 2019). Multiple studies inducing lesions within the DA diencephalic region in amphibians and other vertebrate species have also demonstrated full capability of regeneration (Parish et al., 2007). More interestingly, depending on the specific DA nuclei, regenerative capacity has been shown to vary, and this is likely due to functional differences (Caldwell et al., 2019). Secondly, the results show that there was an initial decline

in the number of PTar/PTac cells in both dominants and subordinates compared to communal animals (Figure 2F, day 7). It is likely that prior social isolation or the initial pairing period of 7 days may have been equally stressful on paired animals. As dominance matures, dominants would recover after a week of social interactions, but subordinates continue to experience social stress (Figure 2F). Indeed, Tea and colleagues (2019) showed that 96 hours of social interactions induces social stress and reduces cell proliferation in the telencephalon of subordinate zebrafish compared to dominants, and this reduction was mediated by increased levels of cortisol (Tea et al., 2019). Interestingly, cortisol levels in dominants were also elevated relative to communally housed fish with significant reduction in cell proliferation in the ventral nucleus of ventral telencephalic area. This suggests that social interactions initially induce stress in the emerging dominant and subordinate fish during the early period of dominance formation with diverging effects on the rate of cell proliferation. Although direct physiological measurement of stress (e.g., cortisol) was not measured in our study; hyperventilation and frequent bottom dwelling of subordinates during the two of pairing is indicative of anxiety-like and stressful behavior consistent with prior reports (Cachat et al., 2010; Demin et al., 2021; Pancotto et al., 2018). Irrespective of which one of these two scenarios is the leading factor, our results suggest that differences in PT cell number might also be a result of socially induced cellular loss. Indeed, the effect of stress induced experimentally via electric shocks or social manipulation has been extensively documented in many other social animals with detrimental consequences on brain morphological and functional organization (Ivy et al., 2010; McEwen et al., 2016; Patel et al., 2018). Finally, it is possible that differences in cell number may be due to a shift in cellular identity whereby dopaminergic neurons can downregulate dopamine synthesis and upregulate glutamate (Demarque and Spitzer, 2012). Recent evidence showed that zebrafish PTar/PTac dopaminergic neurons co-express glutamate synthesizing enzymes (Altbürger et al., 2024). Although we have no evidence to support this view, the apparent increase and decrease in PTar/PTac cell number in dominants and subordinates, respectively, could be due to a shift of DA/glutamate expression. However, it remains undetermined whether the PTar/PTac cells possess the cellular capability of shifting their neurotransmitter identity. Coupled with changes in cell number, our results also show status-dependent synaptic plasticity of the PTar/PTac cells. Subordinates had a higher number of PTar/PTac cells expressing PSD-95 compared to dominants and communals (Figure 4). The functional consequences of increased synaptic formation in subordinates remains unresolved, but it may serve to increase PTar/PTac cellular interconnectivity as a compensatory mechanism to maintain network functionality despite an overall reduction in cell number. Additionally, our results show increased PS6 expression in dominants relative to subordinates, which is consistent with Clements and colleagues' finding showing elevated dopaminergic activities in dominants to regulate the M-cell excitability (Clements et al., 2023). However, we note that elevated levels of PS6 is not necessarily indicative of higher levels of electrical excitability, but

the results suggest that PTN cells are more active biochemically in the synthesis of new proteins that may increase neural excitability.

Our results show that the morphological differences in PT cell number and synaptic density are socially induced and are not due to innate differences. When subordinates were provided the opportunity for social ascent, they quickly adapted their motor activity to reflect dominant status by reducing their startle sensitivity and increased their swimming activity, which was correlated with a significant increase in PTar/PTac cell number (Figure 3A, B). However, behavioral adaptation and morphological plasticity in PTar/PTac during social descent were less obvious (Figure 3C). Dominant animals that lost their social status and became subordinates did not increase their startle sensitivity, nor did they decrease their swimming to subordinates' levels as predicted. However, dominants that were forced into submission showed a significant decline in PTar/PTac cell number. This suggests reluctance to relinquish dominance status, and the pace of behavioral adaptations and morphological plasticity may not be synchronous. The results suggest that brain nuclei involved in motivation and aggression may undergo physiological plasticity at different rates compared to the PTar/PTac. It is likely that the differences in startle sensitivity and swimming frequency would become more pronounced with extended pairing beyond two weeks once the new dominance order solidifies.

It is noteworthy that subordinates that remained submissive during the second pairing (having been subordinates for a total of 28 days) displayed depressive like behavior whereby their swimming activity declined even more than what was observed during the first 2 weeks. Most remarkably, their startle sensitivity began to shift in the opposite direction and became less sensitive to startle stimuli compared to short-term social subordinates. This phenomenon of learned helplessness has been described extensively as the animals' failure to escape shock induced by uncontrollable aversive events. Seligman and Maier theorized that animals learned that outcomes were independent of their responses, and that this learning undermined efforts to escape (Maier and Seligman, 2016; Seligman and Maier, 1967). Similar occurrence is observed in zebrafish exposed to 3 months of social submission leading to display characteristics of learned helpless with minimal swimming and startle escape response, which is consistent with our current results (Issa and Sanders, unpublished observations). Comparison of the startle escape response sensitivity in 14-days subordinates to those of 28-days long subordinates shows a significant difference (Compare Figure 2C to Figure 3B). 28-days of social submission appears to cause those animals to reduce their startle sensitivity with a further decline, albeit modest, in swimming frequency compared to 14-days social subordinates. The results suggest that extended exposure to social submission beyond 28-days is likely to further amplify and fully manifest the effects of learned helplessness.

Behavioral and cellular plasticity in the startle escape response in other teleost fish species such as cichlid (*Astatotilapia burtoni*) and goldfish (*Carassius auratus*) have also been reported (Medan and Preuss, 2014). As with zebrafish, not only M-cell is modulated by direct

and indirect descending neuromodulatory inputs including serotonin (McLean and Fetcho, 2004; Medan and Preuss, 2014; Pereda et al., 1992; Whitaker et al., 2011), but its sensitivity is also socially regulated, and depends on serotonergic modulation (Whitaker et al., 2021). Interestingly, the response of the M-cell in dominant cichlids is enhanced compared to subordinates (Whitaker et al., 2011), suggesting species-dependent adaption to different ecological forces. In cichlids, body coloration is socially regulated whereby dominants are conspicuously brighter compared to subordinates (Korzan et al., 2008). Thus, despite similarities in brain morphological and functional organization among teloses, differences in selective pressures in body coloration and predations can alter brain plasticity and decision-making networks to optimize survival as an adaptation to differences in social and ecological environment.

In conclusion, this study demonstrates that social status affects the morphological architecture of the PTN involved in regulating spinal motor circuits. Results show social status-dependent differences in cellular plasticity in dopaminergic cell number, synaptic density and PS6 expression that correlate with adaptions in the startle escape and swim behavior during social rise and fall. Collectively, the study highlights the impact of social factors in inducing morphological and functional plasticity, the basic principles of which may inform our understanding of other social species with similar structural and functional brain organization.

Acknowledgement

We thank Drs. Stefan Clemens, Elizabeth Ables and Karen Litwa for feedback; Miranda Setneska, Feliciti Gunter, Emma Tunnell and Amanda Hall for assistance; Dr. Timothy Erickson for providing the Tg(dat:GFP) transgenic line; two anonymous reviewers; Dr. Ariane Peralta for her assistance with principal component analysis R-coding and data interpretation. Supported by the National Science Foundation (award # 1754513).

Conflict of Interest Statement

The authors declare that the research was conducted in the absence of any commercial or financial relationships that could be construed as a potential conflict of interest.

Author's Contributions

Fadi Issa designed research. Faith Heagy, Katie Clements, Carrie Adams, and Elena Blain conducted experiments. Faith Heagy and Fadi Issa wrote the paper.

References

- **Altbürger, C., Rath, M., Armbruster, D. and Driever, W.** (2024). Neurog1 and Olig2 integrate patterning and neurogenesis signals in development of zebrafish dopaminergic and glutamatergic dual transmitter neurons. *Developmental Biology* **505**, 85–98.
- Anderson, E. B., Grossrubatscher, I. and Frank, L. (2014). Dynamic Hippocampal Circuits Support Learning- and Memory-Guided Behaviors. *Cold Spring Harb Symp Quant Biol* **79**, 51–58.
- Brenet, A., Hassan-Abdi, R., Somkhit, J., Yanicostas, C. and Soussi-Yanicostas, N. (2019). Defective Excitatory/Inhibitory Synaptic Balance and Increased Neuron Apoptosis in a Zebrafish Model of Dravet Syndrome. *Cells* 8, 1199.
- Cachat, J., Stewart, A., Grossman, L., Gaikwad, S., Kadri, F., Chung, K. M., Wu, N., Wong, K., Roy, S., Suciu, C., et al. (2010). Measuring behavioral and endocrine responses to novelty stress in adult zebrafish. *Nat Protoc* 5, 1786–1799.
- Caldwell, L. J., Davies, N. O., Cavone, L., Mysiak, K. S., Semenova, S. A., Panula, P., Armstrong, J. D., Becker, C. G. and Becker, T. (2019). Regeneration of dopaminergic neurons in adult zebrafish depends on immune system activation and differs for distinct populations. *J Neurosci* 39, 4694–4713.
- Chen, T. J. H., Blum, K., Mathews, D., Fisher, L., Schnautz, N., Braverman, E. R., Schoolfield, J., Downs, B. W. and Comings, D. E. (2005). Are dopaminergic genes involved in a predisposition to pathological aggression? Hypothesizing the importance of "super normal controls" in psychiatric genetic research of complex behavioral disorders. *Med Hypotheses* 65, 703–707.
- Clemens, S., Rye, D. and Hochman, S. (2006). Restless legs syndrome: revisiting the dopamine hypothesis from the spinal cord perspective. *Neurology* **67**, 125–130.
- Clements, K. N., Miller, T. H., Keever, J. M., Hall, A. M. and Issa, F. A. (2018). Social status-related differences in motor activity between wild-type and mutant zebrafish. *Biol Bull* 235, 71–82.
- Clements, K. N., Ahn, S., Park, C., Heagy, F. K., Miller, T. H., Kassai, M. and Issa, F. A. (2023). Socially mediated shift in neural circuits activation regulated by synergistic neuromodulatory signaling. *eNeuro* 10, ENEURO.0311-23.2023.

- **Demarque, M. and Spitzer, N. C.** (2012). Neurotransmitter phenotype plasticity: an unexpected mechanism in the toolbox of network activity homeostasis. *Dev Neurobiol* **72**, 22–32.
- Demin, K. A., Taranov, A. S., Ilyin, N. P., Lakstygal, A. M., Volgin, A. D., de Abreu, M. S., Strekalova, T. and Kalueff, A. V. (2021). Understanding neurobehavioral effects of acute and chronic stress in zebrafish. *Stress* 24, 1–18.
- Edwards, D. H. and Kravitz, E. A. (1997). Serotonin, social status and aggression. *Current opinion in neurobiology* **7**, 812–819.
- **Filby, A. L., Paull, G. C., Hickmore, T. F. and Tyler, C. R.** (2010). Unravelling the neurophysiological basis of aggression in a fish model. *BMC Genomics* **11**, 498.
- Haehnel-Taguchi, M., Fernandes, A. M., Böhler, M., Schmitt, I., Tittel, L. and Driever, W. (2018).

 Projections of the Diencephalospinal Dopaminergic System to Peripheral Sense Organs in Larval Zebrafish (Danio rerio). *Front Neuroanat* 12, 20.
- He, S., Zimmerman, M. W., Layden, H. M., Berezovskaya, A., Etchin, J., Martel, M. W., Thurston, G., Jing, C.-B., van Rooijen, E., Kaufman, C. K., et al. (2021). Synergistic melanoma cell death mediated by inhibition of both MCL1 and BCL2 in high-risk tumors driven by NF1/PTEN loss. *Oncogene* 40, 5718–5729.
- Issa, F. A., O'Brien, G., Kettunen, P., Sagasti, A., Glanzman, D. L. and Papazian, D. M. (2011).
 Neural circuit activity in freely behaving zebrafish (Danio rerio). *Journal of Experimental Biology* 214, 1028–1038.
- Ivy, A. S., Rex, C. S., Chen, Y., Dubé, C., Maras, P. M., Grigoriadis, D. E., Gall, C. M., Lynch, G. and Baram, T. Z. (2010). Hippocampal dysfunction and cognitive impairments provoked by chronic early-life stress involve excessive activation of CRH receptors. *J. Neurosci.* 30, 13005–13015.
- Jung, Y., Kennedy, A., Chiu, H., Mohammad, F., Claridge-Chang, A. and Anderson, D. J. (2020).
 Neurons that Function within an Integrator to Promote a Persistent Behavioral State in
 Drosophila. Neuron 105, 322-333.e5.
- **Kassambara, A. and Mundt, F.** (2020). factoextra: Extract and Visualize the Results of Multivariate Data Analyses.

- **Korn, H. and Faber, D. S.** (2005). The Mauthner cell half a century later: a neurobiological model for decision-making? *Neuron* **47**, 13–28.
- **Korzan, W. J., Robison, R. R., Zhao, S. and Fernald, R. D.** (2008). Color change as a potential behavioral strategy. *Horm Behav* **54**, 463–470.
- **Lindsey, B. W., Douek, A. M., Loosli, F. and Kaslin, J.** (2017). A Whole brain staining, embedding, and clearing pipeline for adult zebrafish to visualize cell proliferation and morphology in 3-Dimensions. *Front Neurosci* **11**, 750.
- Maier, S. F. and Seligman, M. E. P. (2016). Learned helplessness at fifty: Insights from neuroscience. *Psychol Rev* 123, 349–367.
- Manoli, D. S., Meissner, G. W. and Baker, B. S. (2006). Blueprints for behavior: genetic specification of neural circuitry for innate behaviors. *Trends Neurosci* 29, 444–451.
- **Marsden, K. C. and Granato, M.** (2015). In Vivo Ca(2+) imaging reveals that decreased dendritic excitability drives startle habituation. *Cell Rep* **13**, 1733–1740.
- Maruska, K. P., Butler, J. M., Field, K. E., Forester, C. and Augustus, A. (2020). Neural activation patterns associated with maternal mouthbrooding and energetic state in an African cichlid fish. *Neuroscience* **446**, 199–212.
- McEwen, B. S., Nasca, C. and Gray, J. D. (2016). Stress effects on neuronal structure: hippocampus, amygdala, and prefrontal cortex. *Neuropsychopharmacology* 41, 3–23.
- McLean, D. L. and Fetcho, J. R. (2004). Relationship of tyrosine hydroxylase and serotonin immunoreactivity to sensorimotor circuitry in larval zebrafish. *J Comp Neurol* **480**, 57–71.
- **Medan, V. and Preuss, T.** (2014). The Mauthner-cell circuit of fish as a model system for startle plasticity. *J Physiol Paris* **108**, 129–140.
- Miller, T. H., Clements, K., Ahn, S., Park, C., Hye Ji, E. and Issa, F. A. (2017). Social status-dependent shift in neural circuit activation affects decision making. *J Neurosci* 37, 2137–2148.
- Mu, Y., Li, X., Zhang, B. and Du, J. (2012). Visual input modulates audiomotor function via hypothalamic dopaminergic neurons through a cooperative mechanism. *Neuron* 75, 688–699.

- Müller, M. S., Brennecke, J. F., Porter, E. T., Ottinger, M. A. and Anderson, D. J. (2008). Perinatal androgens and adult behavior vary with nestling social system in siblicidal boobies. *PLoS One* 3, e2460.
- **O'Connell, L. A. and Hofmann, H. A.** (2011). The vertebrate mesolimbic reward system and social behavior network: a comparative synthesis. *J Comp Neurol* **519**, 3599–3639.
- O'Connell, L. A. and Hofmann, H. A. (2012a). Social status predicts how sex steroid receptors regulate complex behavior across levels of biological organization. *Endocrinology* **153**, 1341–1351.
- O'Connell, L. A. and Hofmann, H. A. (2012b). Evolution of a vertebrate social decision-making network. *Science* **336**, 1154–1157.
- Oliveira, R. F., Silva, J. F. and Simões, J. M. (2011). Fighting zebrafish: characterization of aggressive behavior and winner-loser effects. *Zebrafish* 8, 73–81.
- Orr, S. A., Ahn, S., Park, C., Miller, T. H., Kassai, M. and Issa, F. A. (2021). Social experience regulates endocannabinoids modulation of zebrafish motor behaviors. *Front Behav Neurosci* 15, 668589.
- Pancotto, L., Mocelin, R., Marcon, M., Herrmann, A. P. and Piato, A. (2018). Anxiolytic and antistress effects of acute administration of acetyl-L-carnitine in zebrafish. *PeerJ* 6, e5309.
- Parish, C. L., Beljajeva, A., Arenas, E. and Simon, A. (2007). Midbrain dopaminergic neurogenesis and behavioural recovery in a salamander lesion-induced regeneration model. *Development* 134, 2881–2887.
- **Patel, D., Anilkumar, S., Chattarji, S. and Buwalda, B.** (2018). Repeated social stress leads to contrasting patterns of structural plasticity in the amygdala and hippocampus. *Behavioural Brain Research* **347**, 314–324.
- Pereda, A., Triller, A., Korn, H. and Faber, D. S. (1992). Dopamine enhances both electrotonic coupling and chemical excitatory postsynaptic potentials at mixed synapses. *Proc Natl Acad Sci U S A* 89, 12088–12092.
- R Code Team (2024). R: A language and environment for statistical computing.

- **Ruvinsky, I. and Meyuhas, O.** (2006). Ribosomal protein S6 phosphorylation: from protein synthesis to cell size. *Trends Biochem Sci* **31**, 342–348.
- Ryczko, D., Grätsch, S., Auclair, F., Dubé, C., Bergeron, S., Alpert, M. H., Cone, J. J., Roitman, M. F., Alford, S. and Dubuc, R. (2013). Forebrain dopamine neurons project down to a brainstem region controlling locomotion. *Proc Natl Acad Sci U S A* 110, E3235-3242.
- Schmidt, R., Strähle, U. and Scholpp, S. (2013). Neurogenesis in zebrafish from embryo to adult. Neural Dev 8, 3.
- Schwab-Reese, L. M., Parker, E. A. and Peek-Asa, C. (2020). The interaction of dopamine genes and financial stressors to predict adulthood intimate partner violence perpetration. *J Interpers Violence* 35, 1251–1268.
- Seligman, M. E. and Maier, S. F. (1967). Failure to escape traumatic shock. J Exp Psychol 74, 1–9.
- **Stagkourakis, S., Spigolon, G., Liu, G. and Anderson, D. J.** (2020). Experience-dependent plasticity in an innate social behavior is mediated by hypothalamic LTP. *Proc Natl Acad Sci U S A* **117**, 25789–25799.
- **Tang, Y., Horikoshi, M. and Li, W.** (2016). ggfortify: Unified Interface to Visualize Statistical Results of Popular R Packages. *The R Journal* **8**, 474–485.
- **Tea, J., Alderman, S. L. and Gilmour, K. M.** (2019). Social stress increases plasma cortisol and reduces forebrain cell proliferation in subordinate male zebrafish (Danio rerio). *Journal of Experimental Biology* **222**, jeb194894.
- **Teles, M. C. and Oliveira, R. F.** (2016). Quantifying aggressive behavior in zebrafish. *Methods in molecular biology (Clifton, N.J.)* **1451**, 293–305.
- **Vernier, P. and Wullimann, M. F.** (2009). Evolution of the Posterior Tuberculum and Preglomerular Nuclear Complex. In *Encyclopedia of Neuroscience* (ed. Binder, M. D.), Hirokawa, N.), and Windhorst, U.), pp. 1404–1413. Berlin, Heidelberg: Springer.
- Wayne, C. R., Karam, A. M., McInnis, A. L., Arms, C. M., Kaller, M. D. and Maruska, K. P. (2023). Impacts of repeated social defeat on behavior and the brain in a cichlid fish. *Journal of Experimental Biology* **226**, jeb246322.

- Weitekamp, C. A., Nguyen, J. and Hofmann, H. A. (2017). Social context affects behavior, preoptic area gene expression, and response to D2 receptor manipulation during territorial defense in a cichlid fish. *Genes, brain, and behavior* 16, 601–611.
- Whitaker, K. W., Neumeister, H., Huffman, L. S., Kidd, C. E., Preuss, T. and Hofmann, H. A. (2011). Serotonergic modulation of startle-escape plasticity in an African cichlid fish: a single-cell molecular and physiological analysis of a vital neural circuit. *J Neurophysiol* **106**, 127–137.
- Whitaker, K. W., Alvarez, M., Preuss, T., Cummings, M. E. and Hofmann, H. A. (2021). Courting danger: socially dominant fish adjust their escape behavior and compensate for increased conspicuousness to avian predators. *Hydrobiologia* 848, 3667–3681.
- Wickham, H. (2016). ggplot2: Elegant Graphics for Data Analysis. Springer International Publishing.
- Yamamoto, K., Bloch, S. and Vernier, P. (2017). New perspective on the regionalization of the anterior forebrain in Osteichthyes. *Development, Growth & Differentiation* **59**, 175–187.
- Yavas, E., Gonzalez, S. and Fanselow, M. S. (2019). Interactions between the hippocampus, prefrontal cortex, and amygdala support complex learning and memory. *F1000Res* **8**, F1000 Faculty Rev-1292.

Figures and Tables

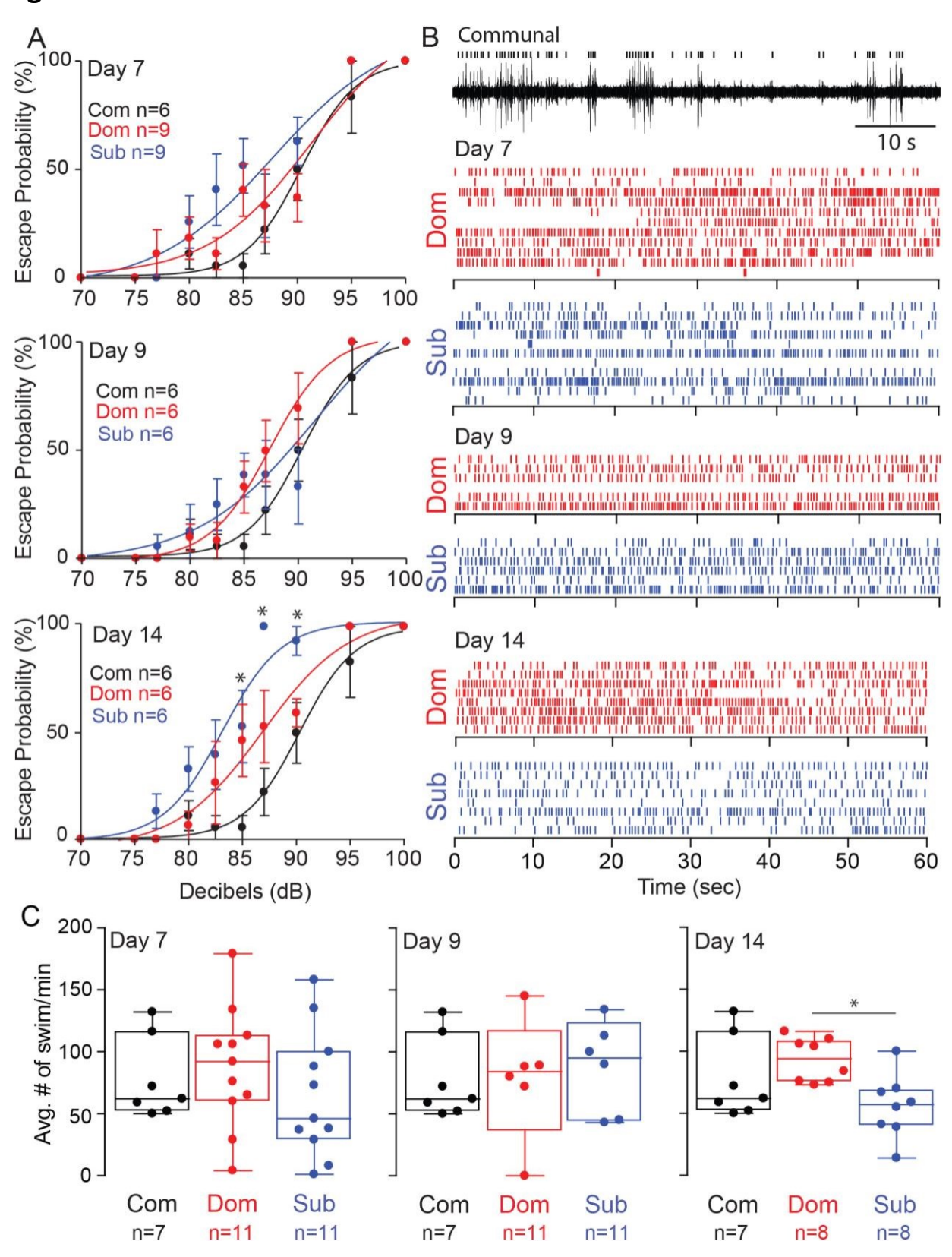


Fig. 1. Effect of social status on startle response and swim behaviors. A-C, startle response probabilities of communals, dominants, and subordinates, on days 7, 9, and 14 of social pairing (left column) along with a corresponding raster plots of swim bursts activity in dominants and subordinates (right column) (communal control data not shown, refer to panel E for a summary of communal). Each row represents the activity of individual fish, and each circle represents one swim burst (top trace is a representation of a raw far-field potential recording from a communal fish). **D**, summary graphs of the average swim bursts per minute among all three social groups. Dots represent average individual fish spontaneous swim activity during a 1-min recording.

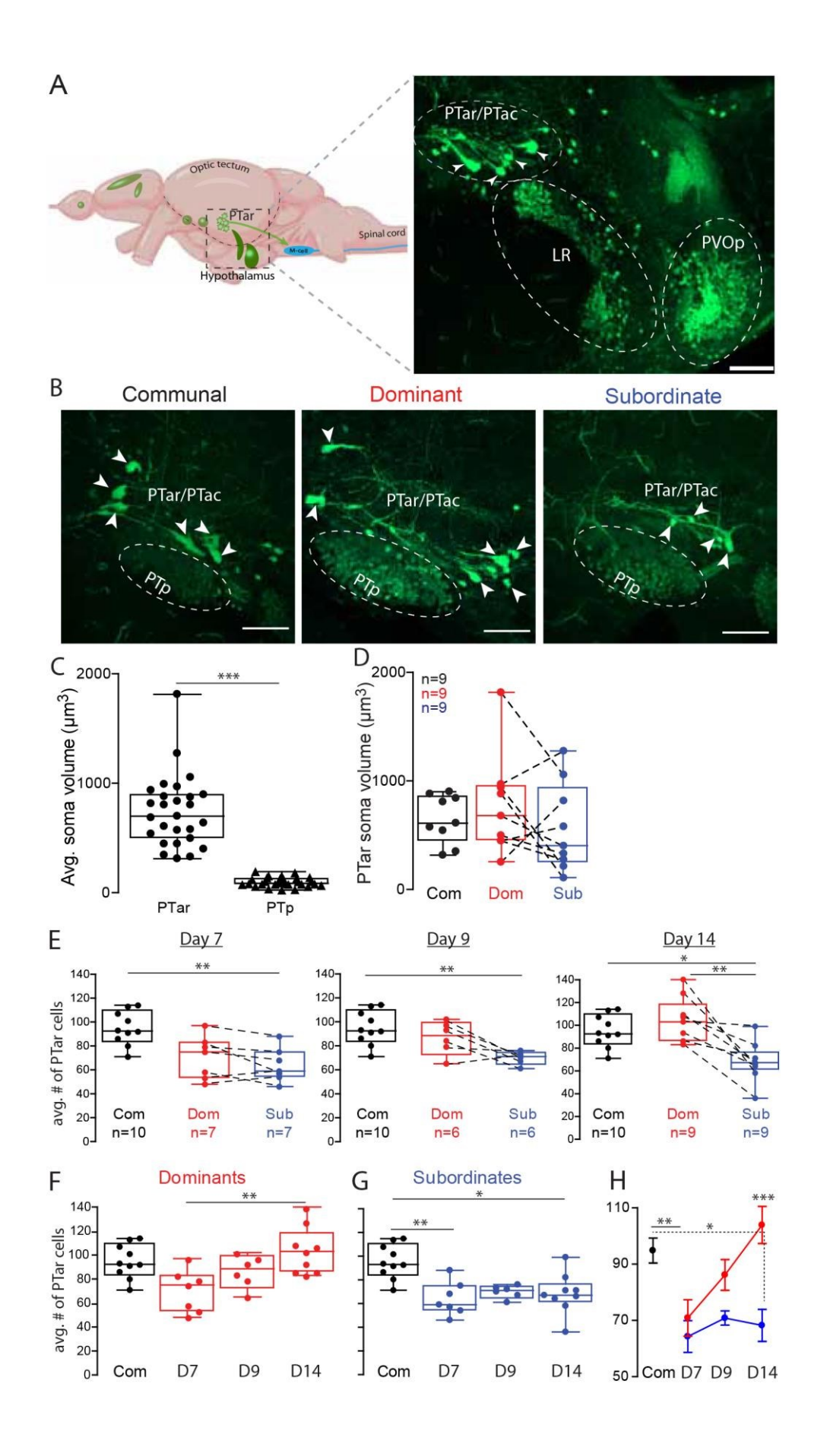
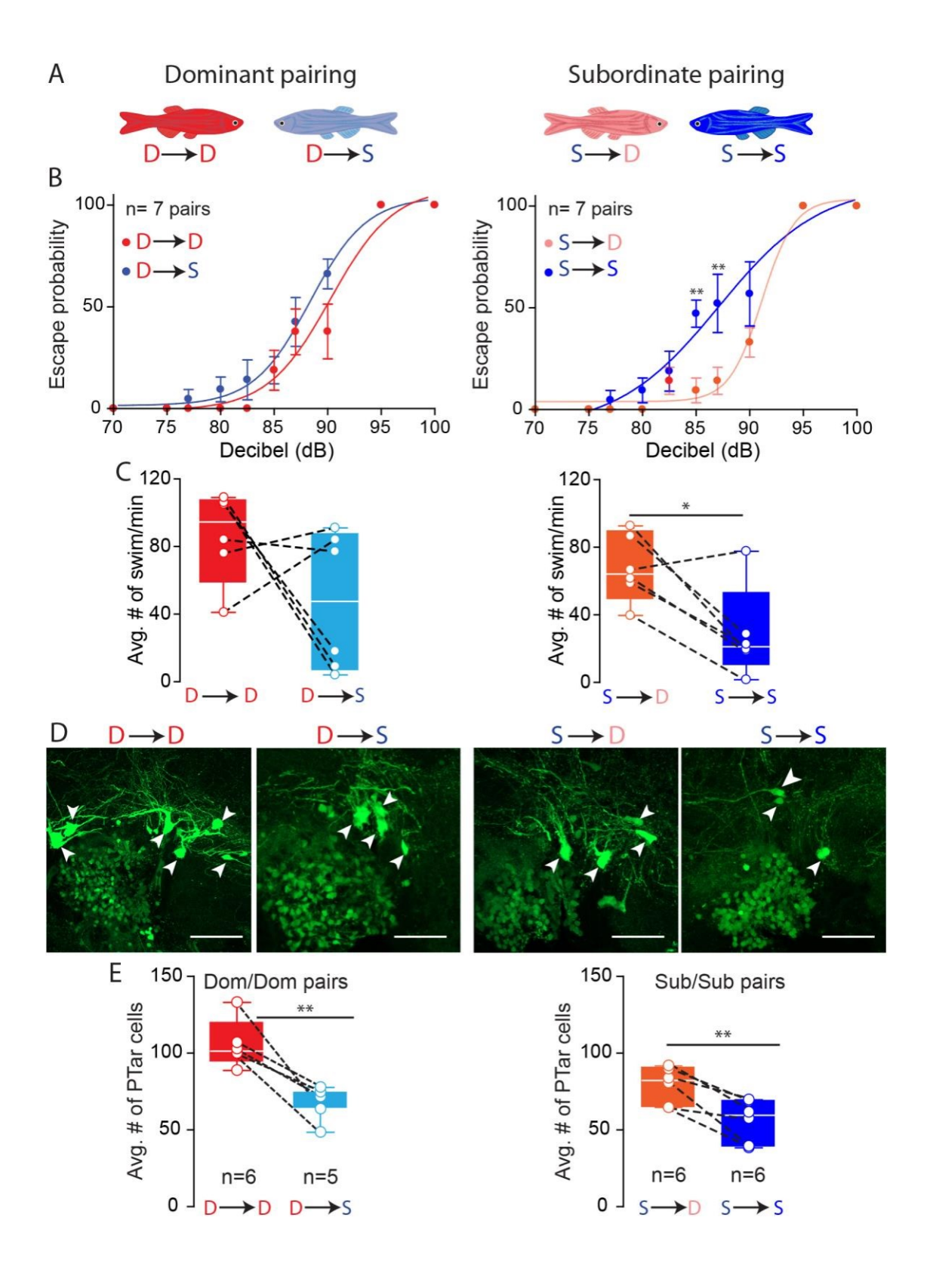
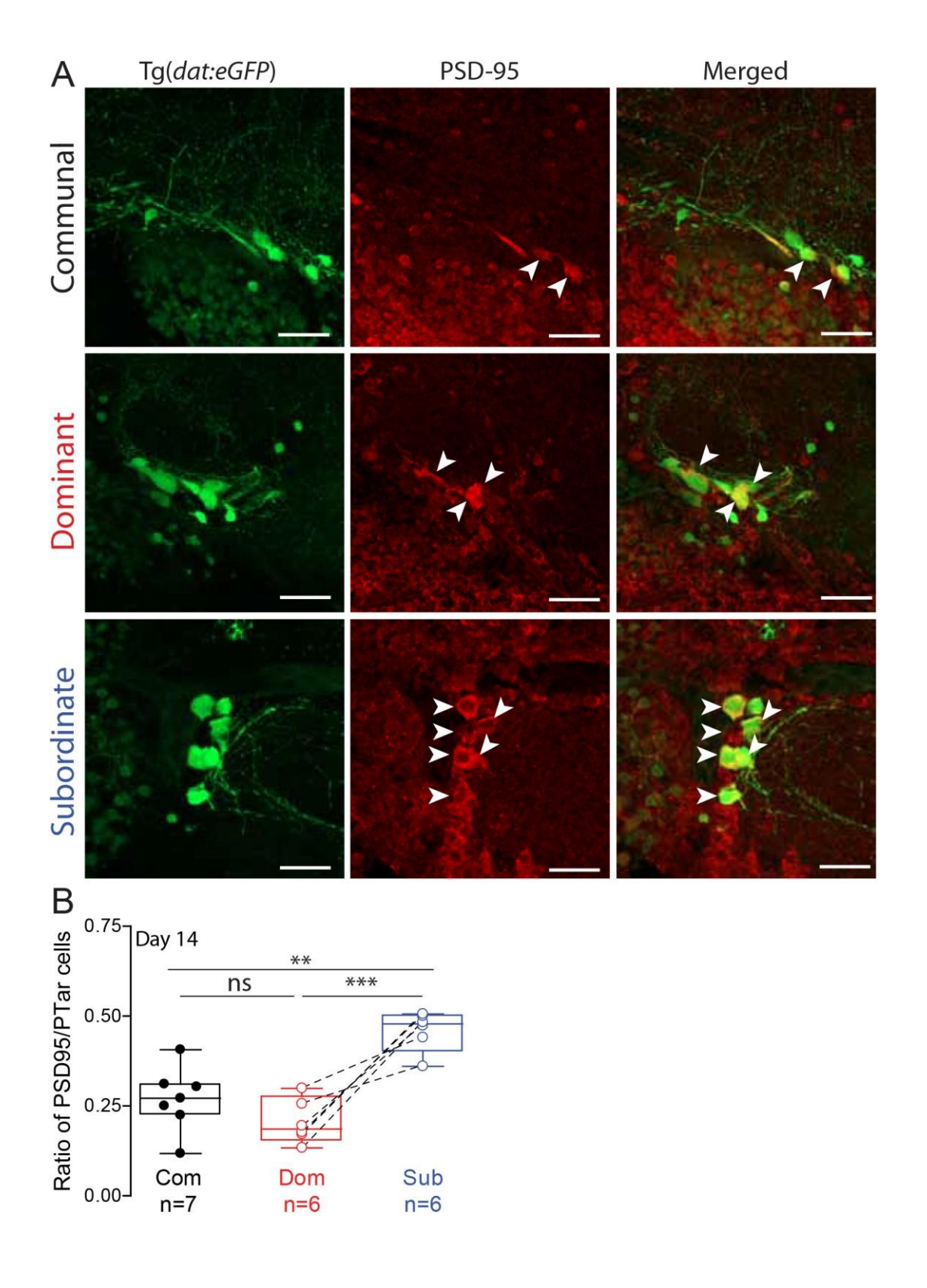


Fig. 2. Effect of social status on PT cell number. **A,** schematic sagittal view of zebrafish approximate DA nuclei and a confocal projection of hypothalamic DA nuclei including the PTar/PTac cluster, lateral recess (LR), PVOp (30 μm thickness) in relation to the Mauthner neuron. **B,** representative confocal projections from a communal, dominant, and subordinate animals highlighting the PTar/PTac somata (arrowheads) and PTp DAT expressing cells (ovals) at 14 days post pairing (scale = 30μm). **C,** average soma volumes for PTar/PTac and PTp cells in communal animals. **D,** Box plot comparison of PTar soma volume across social groups. Dashed lines denote paired-wise comparison of each dominant to its subordinate counterpart. Box denotes 95% of data, horizontal line within the box denotes median, error bars denote minimum and maximum values. **E,** average number of PTar cells on days 7, 9 and 14. **F-H,** same data as shown in panel E but comparing time course changes in the average number of cells separately for dominants and subordinates relative to communals.



ournal of Experimental Biology • Accepted manuscript

Fig. 3. Effect of social reversal on startle sensitivity, swim activity, and PT cell number. A, schematic illustration of experimental crossings (refer to methods for details). D: dominant, S: subordinate. B, startle escape probability in dominant vs. dominant pairs (left), subordinate vs. subordinate pairs (right). C, average number of swim bursts per minute in dominant pairs (left) and subordinate pairs (right). D, representative confocal projections of dominants and subordinates from the (Dom vs Dom) pairs and (Sub vs Sub) pairs. Arrowheads: PTar cells (Scale = $30 \mu m$). E, average number of PTar/PTac cells from the respective animal crossings. Dashed lines denote paired-wise comparison of each dominant to its subordinate counterpart.



ournal of Experimental Biology • Accepted manuscript

Fig. 4. Effect of social status on synaptic connection in PTar nucleus. **A**, representative confocal projections of PTar stained with PSD-95 in Tg(dat:GFP) communal, dominant and subordinate fish (scale = 30 μ m). Arrowheads denote PTar PSD-95 expressing cells. **B**, box plot of the fraction of PTar cells with axosomatic PSD-95 expression. Dashed lines denote paired-wise comparison of each fish with its counterpart.

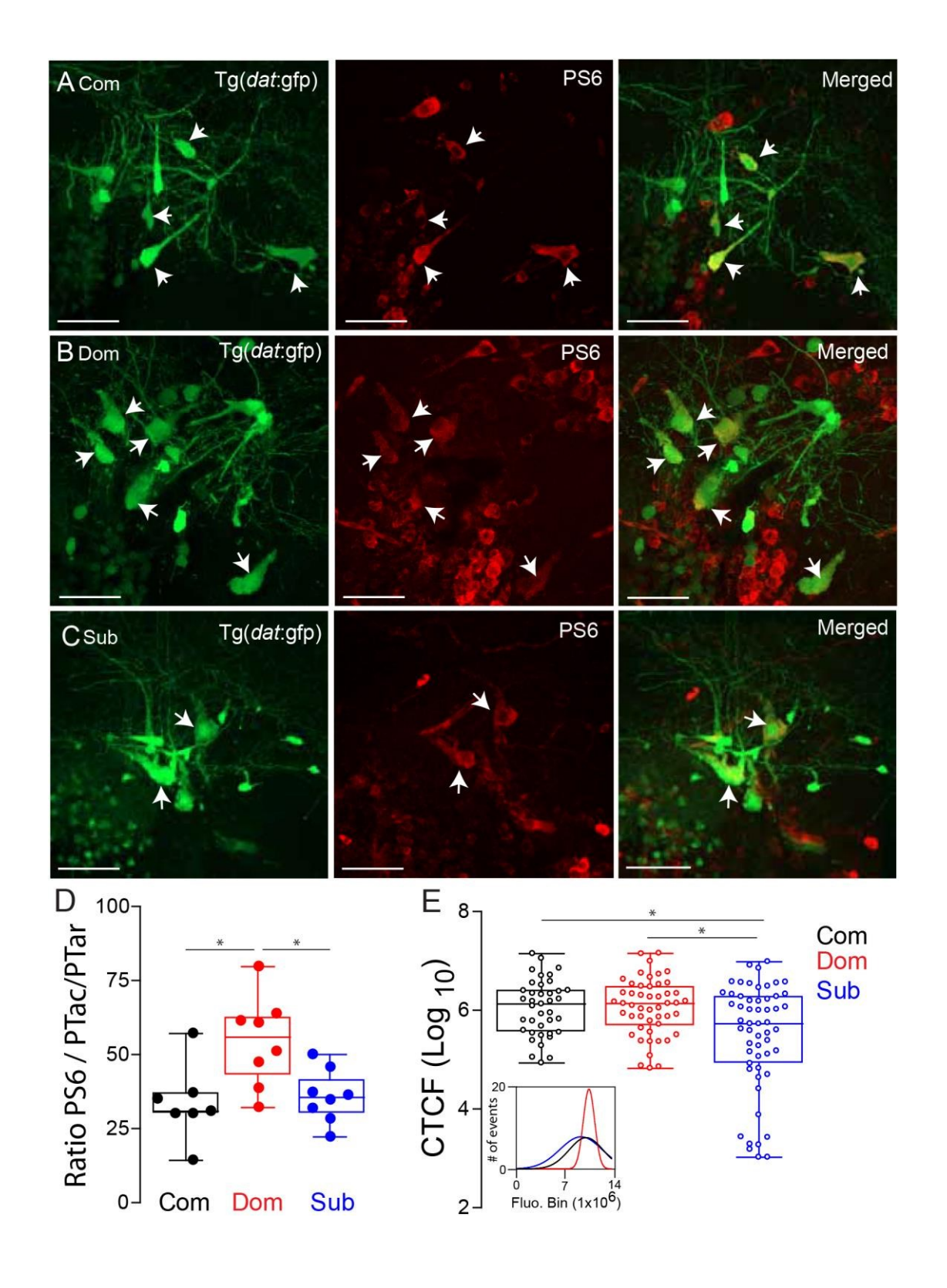


Fig. 5. Effect of social dominance on PS6 expression in PTar/PTac neural cluster. Representative confocal projections of PTar/PTac cluster stained for PS6 in Tg(dat:GFP) communal (A), dominant (B) and subordinate (C) zebrafish (scale = 30 μ m). Arrowheads denote PTar/PTac expressing PS6 somata. D, box plot of the fraction of PTar/PTac cells with PS6 expression. E, box plots of PS6 fluorescence intensity measurements of all PTar/PTac cells analyzed. Inset illustrates the fluorescence intensity frequency distribution.

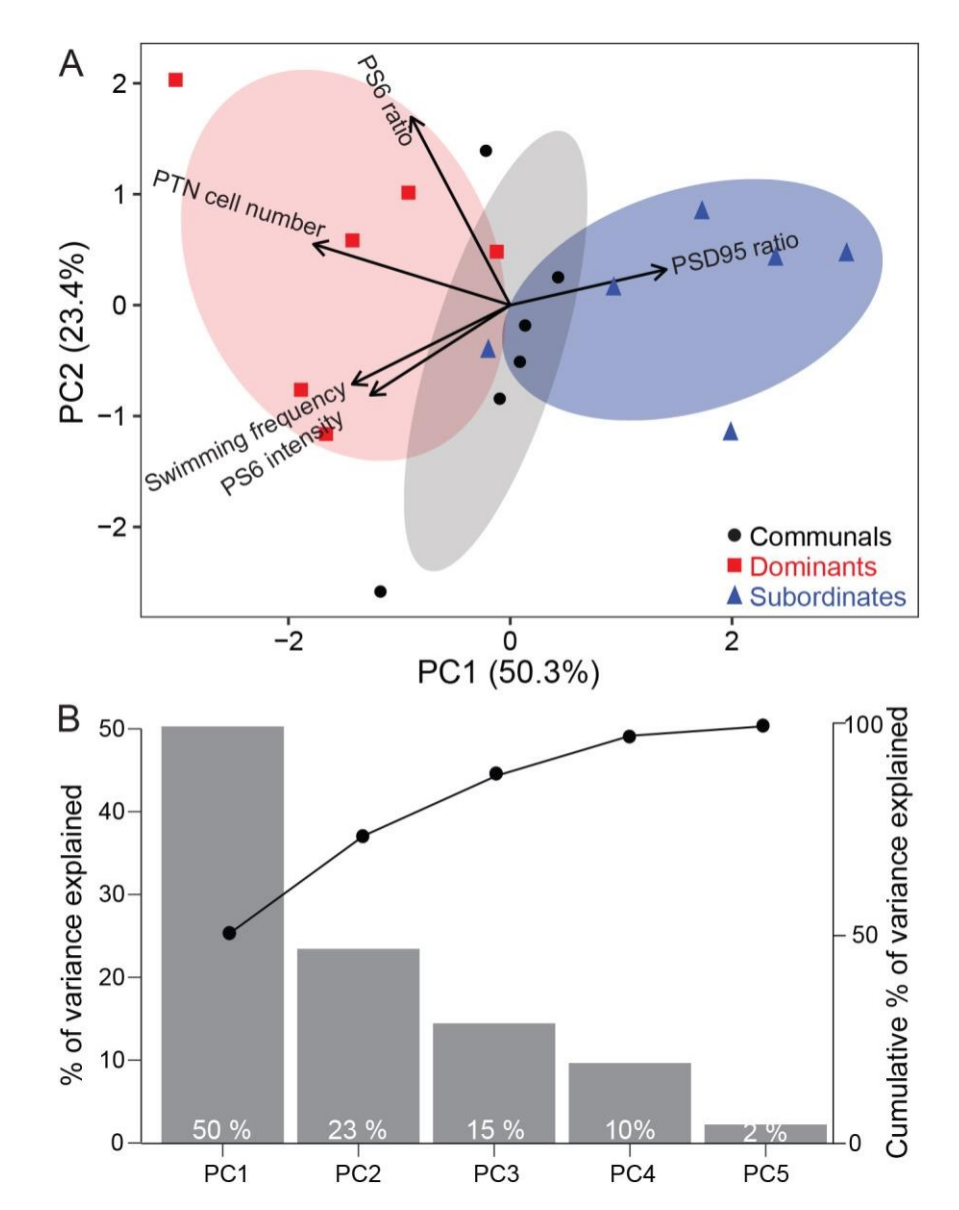
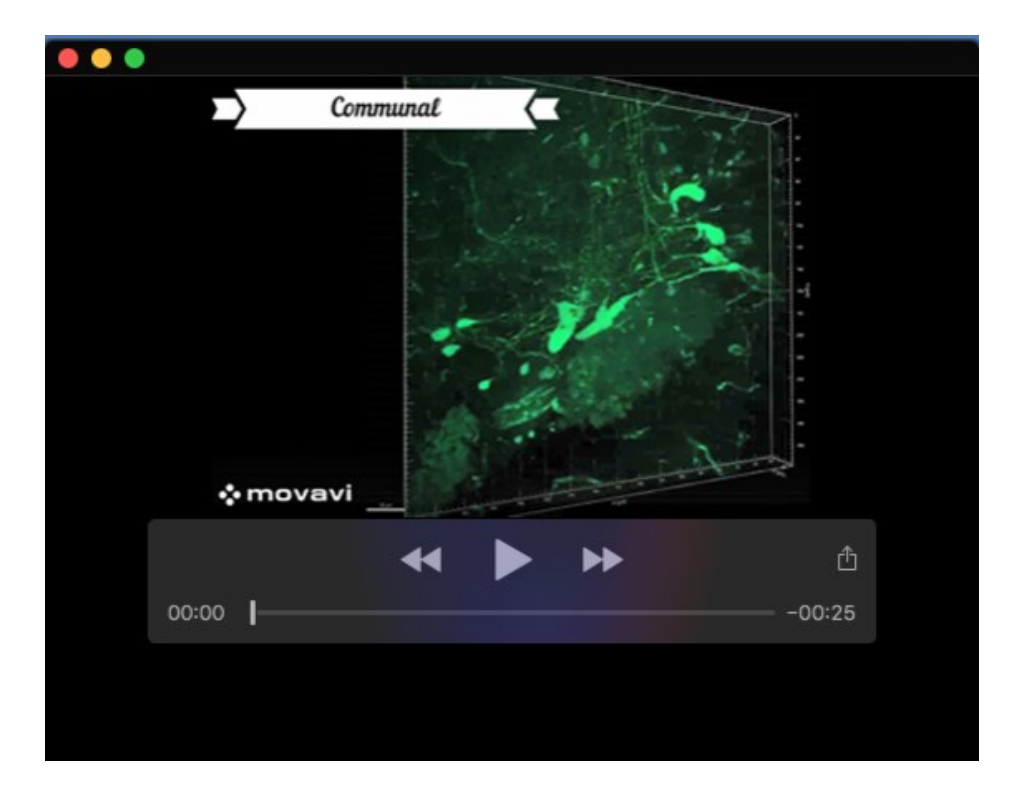


Fig. 6. Ordination based on a Principal Coordinates Analysis depicting swimming frequency, PTN cell number, PS6 and PSD-95 expression according to social status on day 14. (A) PC1 and PC2 are the first and the second Principal components. Points represent samples (6 replicates per social condition), different colors and symbols represent different groups. Ellipses represent 68% confidence intervals of core regions. Loading vectors represent original variables, the directions of arrows represent correlation between original variable and principal components, lengths represent association of original data to principal components. (B) Eigenvalues of the principal components illustrating the amount of variation explained by each component. The plot is arranged so that the eigenvalues are listed in descending order, from the highest to the lowest. Line plot illustrate the cumulative explained variance.

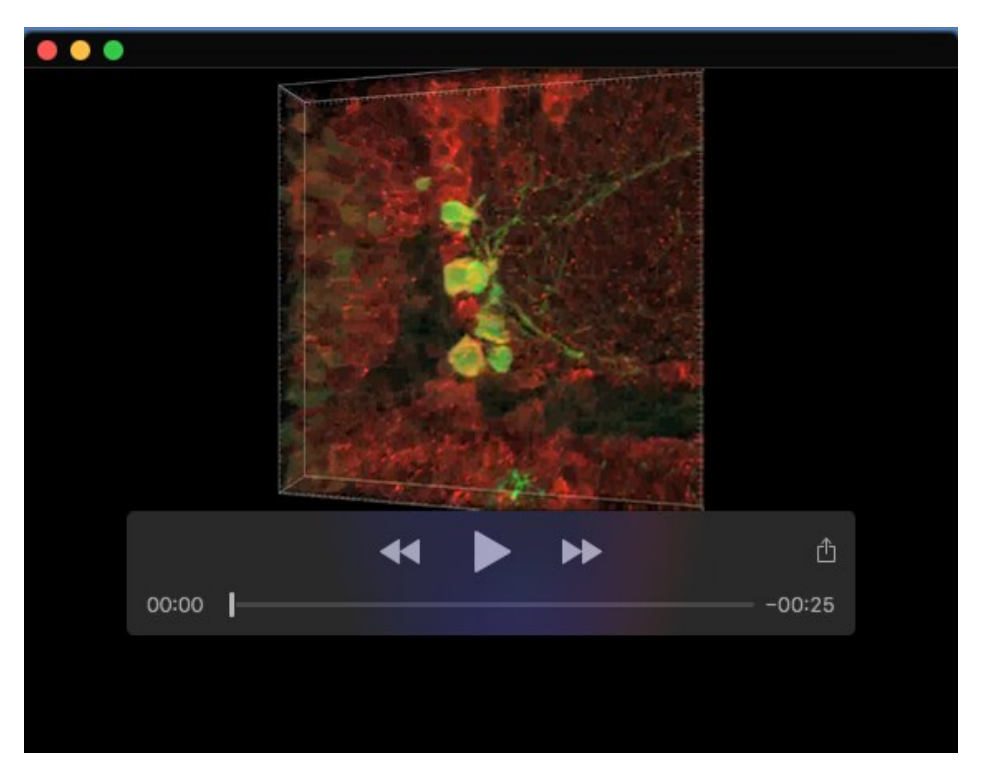
Journal of Experimental Biology • Accepted manuscript

Table 1. Means ± SD are shown. One-way ANOVA with Kruskal-Wallis multiple comparison posttest. n indicates number of animals analyzed.

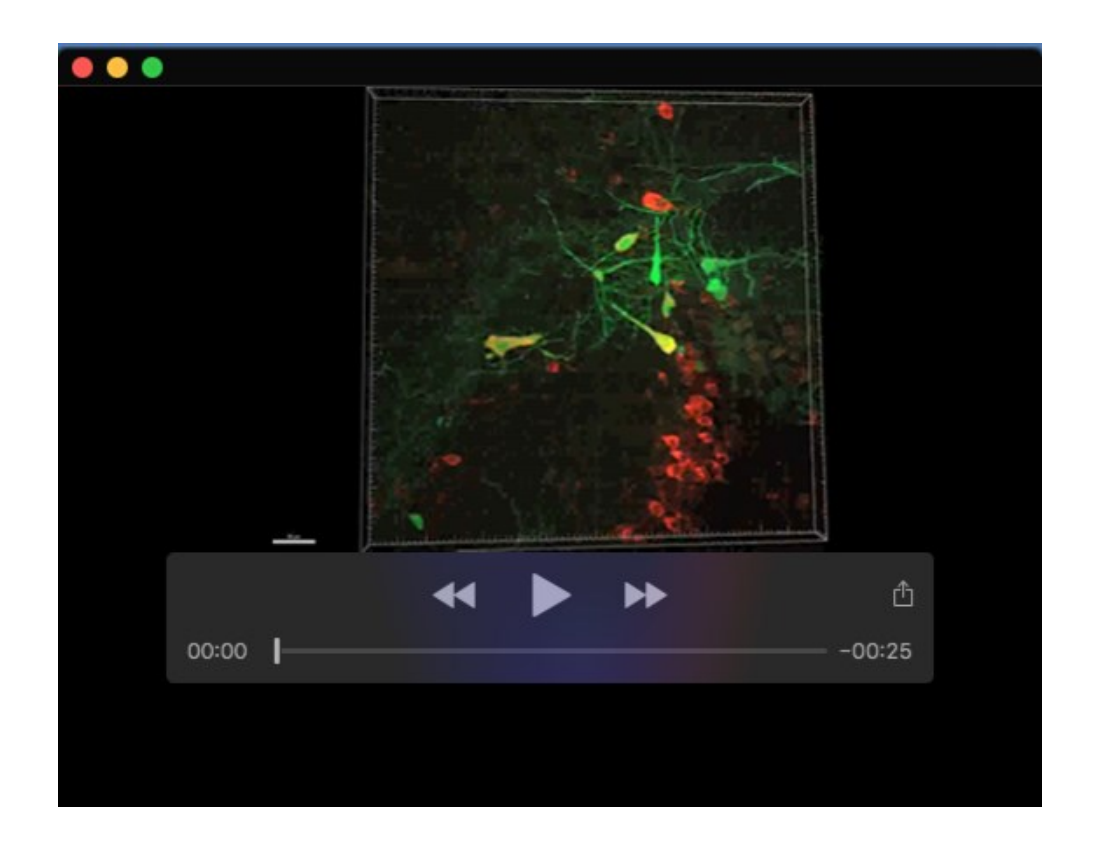
| | Communals | Dominants (n=7) | Subordinates | One-way |
|----------------|--------------|-----------------|--------------|---------------|
| | (n=10) | | (n=7) | ANOVA P value |
| Lateral recess | 528.5 ±163.5 | 620 ±82 | 441 ±111 | 0.0578 |
| PVOp | 4586 ±942 | 5248 ±1067 | 4799 ±1207 | 0.4434 |



Movie 1. 3D projections of confocal images illustrating the DAT:gfp expressing hypothalamic PTar/PTac and PTp nuclei along with somata digital rendering taken from a communal (clip 1), dominant (clip 2), and subordinate (clip 3) zebrafish. PTar/PTac surface rendering illustrated in red, and PTp somata are illustrated in blue.



Movie 2. 3D projections of confocal images illustrating the co-expression of PSD-95 (red) in DAT+ PTar/PTac soma (green) taken from a subordinate zebrafish.



Movie 3. 3D projections of confocal images illustrating the co-expression of PS6 (red) in DAT+ PTar/PTac soma (green) taken from a communal zebrafish. Yellow channel shows the co-localized expressing cells.